# A Decade of Changing Net Radiation over a Large Lake: Remote Sensing Approach for Water - Atmosphere Parameterizations

Pakorn Petchprayoon
Geo-Informatics and Space Technology Development Agency, Bangkok, Thailand
Email: pakorn@gistda.or.th

Peter D. Blanken, Khalid Hussein, Waleed Abdalati
University of Colorado at Boulder, Boulder, USA
Email: blanken@colorado.edu, khalid.hussein@colorado.edu, waleed.abdalati@colorado.edu

***Abstract*—This study uses eleven years (2002-2012) of daily remotely-sensed data with multi-spatial resolution of 1 km to 5 km to examine the spatiotemporal distribution of net radiation ($Q^*$) and its four components: incoming shortwave (K↓), outgoing shortwave (K↑), incoming long-wave (L↓), and outgoing long-wave (L↑) under all sky conditions across Lake Huron. Good agreement was found between the in-situ measurements of net radiation components and instantaneous estimates made from the satellite data with correlation coefficients between 0.95 and 0.60 for outgoing long-wave radiation and incoming shortwave radiation, respectively. Results showed that Q* and all of its components significantly changed over the study period. Trend analysis revealed a significant decrease in Q* at the rate of 0.003 $Wm^{-2}$ $day^{-1}$ with a significant decrease in shortwave (K↓ and K↑), and a significant increase in long-wave (L↓ and L↑). The positive trend of outgoing long-wave radiation was a result of the increase of surface water temperature. The possible reason of reducing surface incoming shortwave radiation was mainly due to the increase of energy absorption by water vapor in the atmosphere.**

*Index Terms*—**Remote Sensing, Net Radiation, Great Lakes,**

## I. INTRODUCTION

### A. Statement of Problem

The surface net radiation ($Q^*$) is the algebraic sum of the four radiation components [1] including: 1) the incoming, downward, shortwave radiation from the Sun and sky ($K\downarrow$), 2) the outgoing shortwave radiation, the reflected solar radiation ($K\uparrow$), 3) the incoming long-wave, thermal, radiation from the atmosphere ($L\downarrow$), and 4) the outgoing long-wave radiation from the surface ($L\uparrow$). Therefore, net radiation can be expressed as: $Q^* = K\downarrow - K\uparrow + L\downarrow - L\uparrow$.

Net radiation is the key component in understanding the surface energy balance and heat flux interface of the atmosphere [2] [3]. This flux interface is the one of the major determinants of climate. Over large areas, accurate information of spatial and temporal variability of the net radiation and its components are important for regional and global climate models [4].

Point measurements of the surface net radiation and its components can be acquired from meteorological stations. In the North American Great Lakes region, however, there are few over-lake stations and also there are limitations on their footprint, thus, there will never be sufficient flux towers or field measurements network that adequately represent climatological parameters of large areas of the Great Lakes under all conditions. Moreover, in the temporal scale, none such regular long-term instrumental observations exist on the Great Lakes' water surface because of winter severity and a lack of secure research instrument bases [5] [6]. Most available long-term net radiation measurement stations located on or near shore where signals are contaminated by surrounding non-water surfaces. Therefore, with far too sparse and period of off-shore observations, it is impossible to provide a realistic, thorough picture of net radiation that meet the requirement of climate research community.

Satellite remote sensing is most likely the only efficient and practical technique to provide regional to global radiometric observations of critically required inputs for estimating surface radiation components. Regionally and globally-averaged quantities can be estimated without the under-sampling problem inherent in sparse observation networks [7]. Several studies have attempted to calculate net radiation by combining remote sensing observations with in-situ data [8] [9]. Some studies have solely used satellite data to estimate net radiation [10] [11] or some of its components such as net surface shortwave radiation [12], net surface long-wave radiation [13]. All these analyses were focused on a short term (1 or 2 years) over land surface. This study is probably the first time to apply exclusively remotely sensed data to study long-term surface net radiation under all sky conditions over a large water surface.

The purpose of this paper is to estimate the spatial and temporal distribution, as well as, long-term changes in the lake surface net radiation and its four components under all sky conditions using satellite data. The results of this study will be significant and beneficial in understanding the spatial and temporal distribution of net

radiation over a large lake. This will contribute to the climate research communities both at regional and global scales.

### B. Study Area

Lake Huron (Fig. 1) is the second largest of the Great Lakes, with a surface area of 59,600 $km^2$ making it the third largest fresh water lake on Earth. The lake has a volume of 3,540 $km^3$, and a shoreline length of 6,157 km [14]. The mean surface height of Lake Huron is 176 m above sea level. The lake's average depth is 59 m, while the maximum depth is 229 m. It has a length of 332 km and a greatest breadth of 245 km [15].

Spectacle Reef Lighthouse, located 17.22 km east of the eastern end of Bois Blanc Island at 45.7732 N and 84.1367 W, is the only station measuring year-round meteorological variables over the lake. The station uses the eddy covariance method to measure the turbulent heat fluxes (sensible and latent heat), net radiation, air temperature, humidity, rain rate, and lake surface temperature. The lighthouse is the major platform providing the year-round, continuous 30-min average meteorological and fluxes data for calculating and validating net radiation components for this study.

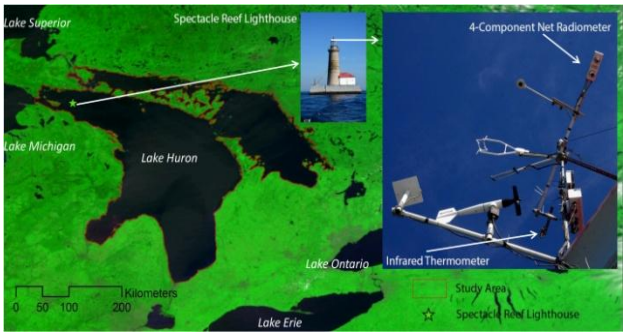


Figure 1. Study area and the location of Spectacle Reef Lighthouse with meteorological instruments (4-Component Net Radiometer, Infrared thermometer).

## II. DATA

### A. Satellite Data

Measurement of net radiation and its components were obtained throughout the period between 2002 and 2012. Four MODIS data products including: MOD03 (geological product), MOD06 (cloud product), MOD07 (atmospheric profile product), and MOD11 (land surface temperature product) were used. These data were in Hierarchical Data Format - Earth Observing System (HDF-EOS) which contains multi-object files. Data were acquired from the National Aeronautics and Space Administration Land Processes Distributed Active Archive Center. All products except MOD11 were extracted and mosaicked using MODIS Conversion Toolkit (MCTK). For MOD11, the thermal images were extracted, reprojected, and mosaicked using MODIS Reprojection Tool [16]. The following table illustrates the characteristics of each product.

TABLE I. MODIS PRODUCTS FOR ESTIMATING NET RADIATION

| Products | Data used (and its Spatial Resolution) | |
|---|---|---|
| MOD03 | Solar zenith angles | (1 km) |
| MOD06 L2 | Cloud optical thickness | (5 km) |
| | Cloud top temperature | (5 km) |
| | Cloud emissivity | (5 km) |
| | Cloud fraction | (5 km) |
| | Surface temperature | (5 km) |
| MOD07 L2 | Dew temperature | (5 km) |
| | Air temperature | (5 km) |
| MOD11A1 | Daily surface temperature | (1 km) |
| MOD11A2 | 8 days surface temperature | (1 km) |

### B. In-situ Measurements

Ground data from the meteorological station located on the top of Spectacle Reef Lighthouse were used for satellite data validation. The station provides 30 minute averages of a number of observations of net radiation and its four components, which were measured by 4-Component Net Radiometer (model CNR4 Campbell Scientific, Logan, UT). Infrared thermometer (model 4000.4GL, Everest) was used to measure water surface temperature in order to calculate outgoing long-wave radiation. All data recorded by Campbell Scientific CR23X micrologger.

## III. METHODOLOY

All surfaces receive short-wave radiation during the daytime and exchange long-wave radiation continuously with the atmosphere. This exchange determines the net radiation. For this study, net radiation at the water surface can be expressed in terms of its components as:

$$Q^* = (1-\alpha)K\downarrow + L\downarrow - L\uparrow \quad (1)$$

### A. Surface Albedo

In a clear sky, in the absence of diffuse radiation, the reflectivity of the lake's surface can be estimated using solar zenith angle which was obtained from MOD03 Geological product. Fresnel reflection equation for un-polarized radiation [17] was applied. The equation can be written as:

$$\alpha(\theta,n) = \frac{1}{2}\left[\frac{sin^2(\theta-n)}{sin^2(\theta+n)} + \frac{tan^2(\theta-n)}{tan^2(\theta+n)}\right] \quad (2)$$

where: $\theta$ is solar zenith angle, $n$ is the angle of refraction for the medium.

For water:

$$sin\, n = sin\frac{\theta}{m} \quad (3)$$

where: $m$ is the index of refraction (1.33 for visible spectrum region)

Under cloudy sky conditions, albedo values were calculated from field data collected over Great Slave Lake [18]. We did not estimate albedo values directly from Lake Huron in-situ measurements, because the albedo signal was contaminated by the lighthouse's

concrete base, which lead to overestimation of albedo values.

*B. Incoming Shortwave Radiation*

The computation of incoming shortwave radiation for clear sky conditions (W $m^{-2}$) was carried out using two parameters, vapor pressure and solar zenith angle. The method developed by Zillman [19] cited in [10] was used and the equation can be written as:

$$K\downarrow_{\text{Clear}} = \frac{S_0 \cos^2\theta}{1.085\cos(\theta) + e_o(2.7+\cos(\theta)) \times 10^{-3} + \beta} \quad (4)$$

where: $S_o$ is the solar constant 1376 $Wm^{-2}$, $\beta$ is a constant value ( 0.1), $e_o$ is vapor pressure (hPa)

Vapor pressure, $e_o$ (hPa) was estimated from dew point temperature using Clausius-Clapeyron method [20] cited in [10]:

$$e_o = 6.11 \exp\left[\frac{L_v}{R_v}\left(\frac{1}{273.15} - \frac{1}{T_d}\right)\right] \quad (5)$$

where: $L_v$ is the latent heat of vaporization ($2.56 \times 10^6$J $kg^{-1}$), $R_v$ is the constant of gas for water vapor (461 J $kg^{-1}$ $K^{-1}$), $T_d$ is dew point temperature (K).

Dew point temperature ( $T_d$ ) was derived from MOD07 atmospheric profile product. Since, the study area characterized by frequent occurrence of cloudy-sky conditions, particularly in the winter season, shortwave radiation is mostly attenuated by clouds. Therefore, under cloudy sky conditions, we applied the method proposed by Slingo [21], in which the incoming shortwave radiation (W $m^{-2}$) was calculated by weighting the shortwave radiation of clear sky using cloud fraction and cloud optical thickness. These two parameters were obtained from MOD06 cloud product. The equation can be expressed as:

$$K\downarrow_{Cloudy} = K\downarrow_{\text{Clear}} \left[(1 - f_c) + f_c e^{-\tau_c/\cos(\theta)}\right] \quad (6)$$

where: $f_c$ is cloud fraction (no units), $\tau_c$ is cloud optical thickness (no units)

*C. Incoming Longwave Radiation*

Incoming longwave radiation (W $m^{-2}$) under clear-sky conditions were calculated using air temperature and air emissivity with the Stefan-Boltzman law.

$$L\downarrow = \sigma\varepsilon_a T_a^4 \quad (7)$$

where: $T_a$(K) is air temperature at the height of 31 m above the water surface, $\varepsilon_a$ is effective air emissivity (no units), σ is Stefan-Boltzman constant $5.67 \times 10^{-8}$ W $m^{-2}$ $K^{-4}$

Air temperature ( $T_a$ ) was derived from MOD07 Atmospheric profile product. Effective air emissivity was estimated by Prata approach [22]:

$$\varepsilon_a = 1 - (1 + \vartheta)\, exp\left(\sqrt{1.2 + 3\vartheta}\right) \quad (8)$$

where: $\vartheta = \left(\frac{46.5}{T_a}\right) e_0$ (9)

In the case of cloudy conditions, some pixels values of MOD07 were missing (between 40 – 85 % missing value during summer and winter season). Thus, MODIS's surface temperature from MOD06 cloud product was employed to fill in these missing values of dew point temperature and air temperature by calculating temperature offsets. These offsets were computed as the difference between the MOD06 surface temperatures and the *in-situ* data from the Spectacle Reef meteorological station. The difference between surface water temperature and air temperature (dew point temperature) also was not constant year around. The offset was varied with season, particularly during winter, due to the difference in heat capacity between air and water. Thus, this study proposed calculating separate temperature offsets for winter and non-winter season. Then, incoming long-wave radiation during all sky conditions was estimated as a combination of incoming long-wave during clear sky condition and long-wave emitted from clouds.

$$L\downarrow = \sigma\varepsilon_a T_a^4 + \sigma(1 - \varepsilon_a)\varepsilon_c T_c^4 \quad (10)$$

where: $T_c$ is cloud temperature (K), $\varepsilon_c$ is cloud emissivity. Both cloud temperature and cloud emissivity was obtained from MOD06 cloud product

*D. Outgoing Long-wave Radiation*

Outgoing long-wave radiation (W $m^{-2}$) was calculated using MODIS's thermal surface temperature for all sky conditions. Under cloudy sky, MODIS's cloud free data composite image (MOD11A2, 8 days composite product) was employed to fill in these missing value pixels (20-90%). However, it was found that during the winter season, there were some areas where new temperature imagery may not be available for more than 10 days because of cloud cover [23]. To overcome this problem of missing data in both MOD11A1 and MOD11A2, spatial Inverse Distance Weighted (IDW) interpolation technique was used to calculate the missing pixels values of MOD11A2. Then the values of MOD11A2 were used to fill the missing values in daily MODIS data (MOD11A1). However, using MOD11A2 to fill the missing data pixels in MOD11A1 could introduce uncertainty because, the composite MOD11A2 data may be collected at different view angles, on different dates, and under different atmospheric conditions. Thus, it is necessary to validate the data before using them. The emitted long-wave radiation was calculated using the Stefan-Boltzman relationship, which can be written as:

$$L\uparrow = \sigma\varepsilon_s T_s^4 \quad (11)$$

where: $T_s$ is water surface temperature (K), $\varepsilon_s$ is emissivity of water surface

### E. Data Validation

Net radiation and its components were calculated using estimations of water surface and atmospheric parameters from remotely-sensed data. Therefore, the accuracy of these components must be validated with information acquired by the meteorological towers. Satellite data and field measurements gathered during the year of 2010 was used for validation. The ground-based technique that directly evaluates the satellite – derived surface net radiation variable with in-situ direct measurements at the satellite overpass has been applied to validate satellite data over different land cover and land use including large lakes, grasslands, and agricultural fields [24]. The data of the meteorological station on the top of Spectacle Reef Lighthouse, which is positioned far from shoreline, was an ideal data for validation of the satellite data.

## IV. Results and Discussion

### A. Comparison of daily satellite net radiation components to the ground-based observations

The MODIS incoming solar radiation versus direct measurements from pyranometer showed a good agreement. The $R^2$ was 0.77, in clear-sky conditions, 0.70 for all sky condition, and the $R^2$ under cloudy-sky conditions was 0.61. This low correlation coefficient might be due to the effect of the difference in spatial scale between direct measurements and satellites observations. The direct measurement recorded a single point from the meteorological station, whereas each pixel of satellite data record information at a 25 $km^2$ spatial coverage.

An important uncertainty associated with co-location of satellite and ground measurements were temporal and spatial sampling errors. Temporal sampling error arises from the fact that the surface measurement has 30 minutes average incoming shortwave radiation calculated from measurements collected every 5 seconds, while satellite instantaneous capture signals with less than 1 second per pixel. Since, clouds change overtime, 30 minutes different range of record time has a high potential to introduce different amount of incoming shortwave radiation. Spatial sampling error occurs because, MODIS pixel aggregates the radiometric radiation signal from area of 5 x 5 km which is much greater than the pyranometer's field of view. A single small isolated cloud right over the meteorological station considerably reduces the shortwave incoming radiation reached at the pyranometer, whereas producing a small effect on the measurement from the satellite. In contrast, if there were clouds over almost all of the satellite pixel, except over the pyranometer, then the incoming shortwave radiation from surface measurement will be higher than the one from the satellite observation.

Since, the measurements of the reflected solar radiation were affected by the base of the lighthouse structure that could not be avoided, no validation was carried out for outgoing radiation. We understand that for satellite retrieved parameter that is lacking validation of data will introduce more uncertainty in study results, however, the reflected solar radiation was the smallest component of the net radiation (less than 5% of the net radiation).

For the incoming long-wave radiation, the correlation coefficient between these two data sources (MODIS and in situ) were 0.72, 0.60, and 0.64 for clear, cloudy, and all sky conditions, respectively. These low coefficient values were mainly due to the effect of the difference in spatial scale observed and cloud cover impacts as discussed earlier on the incoming shortwave radiation.

Direct measurements of outgoing long-wave radiation were not available because of signal contamination from the lighthouse base, thus measurements of surface water temperature by infrared thermometer were used to calculate the upwelling long-wave using the Stefan-Boltzman relationship assuming constant surface emissivity of 0.97. The correlation coefficients between the calculated and the measured outgoing long-wave radiation were 0.95, 0.91, and 0.93 for clear, cloudy, and all sky condition, respectively. Fig. 2 shows the scatter plot of in situ measurements of three net radiation components (incoming shortwave, incoming long-wave, and outgoing long-wave of net radiation for all sky conditions.

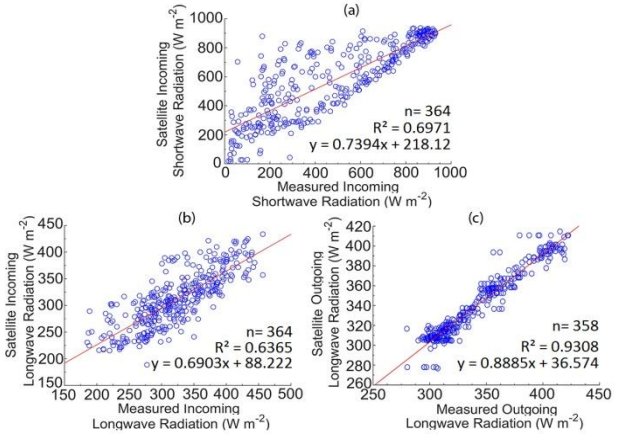


Figure 2. Scatter plot of satellite's net radiation components versus the directly measured data (30 min average) including incoming shortwave (a), incoming long-wave (b), outgoing long-wave (c) for the year 2010.

### B. Temporal and spatial distribution of net radiation

The annual variation and ratio of net radiation and its components is shown in Fig. 3 and Fig. 4. The instantaneous net radiation was dominated by incident shortwave radiation, indicating that daytime radiation budget of the lake surface was remarkably dominated by energy absorption. The ratio of net radiation and incoming shortwave radiation was nearly constant all year around, but the pattern was slightly greater during the wintertime. Outgoing shortwave flux had relatively small value due to very low reflection coefficient of water.

For long-wave radiation, the difference between upward and downward long-wave radiation was also almost constant with positive values between 30 $Wm^{-2}$ (winter) to 50 $Wm^{-2}$ (summer) which was an indication

that the water surface lost more long-wave radiation than it gained all year around. Long-wave radiation (incoming and outgoing) also had less seasonal variation and much lower density than the incoming shortwave radiation, particularly in the summertime which presented the lowest ratio of net radiation and long-wave radiation. In winter, due to the high thermal inertia of lake water and high cloud cover, both downward and upward long-wave radiations were greater than incident shortwave which had the lowest intensity due to the low solar angles and the frequent occurrence of clouds. Therefore, the ratio of long-wave radiation to net radiation was greater during the wintertime.

The spatial distribution of yearly daytime instantaneous surface net radiation over Lake Huron is shown in Fig. 5. In January – April and September – December, the distribution of net radiation had an approximately regular latitudinal pattern which was controlled by solar zenith angle. In March, with the increase in solar elevation, the net radiation increased rapidly which was almost two times greater than the value of February. In April, the net radiation continued to increase but the variation with latitude was not obvious.

From May to August, the spatial distribution of net radiation over the lake did not show the variation with latitude. The variability of net radiation was related to lake's bathymetry and the presence or absence of cloud covers. June was the month of highest net radiation. After this month, the net radiation started to decrease due to decreasing solar elevation. However, the water surface still had a high temperature, which resulted in a greater emission of long-wave radiation. The latitudinal pattern of net radiation spatial distribution started to reconstruct in September and again reached regular latitudinal pattern.

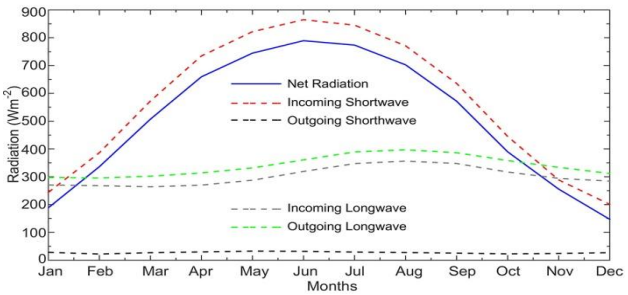


Figure 3. Annual change of net radiation and its components including incoming shortwave, outgoing shortwave, incoming long-wave, and outgoing long-wave over Lake Huron (in $Wm^{-2}$).

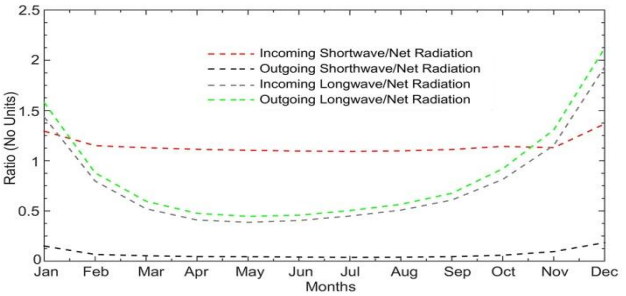


Figure 4. Ratio of each of the net radiation components during the period of 2001-2012

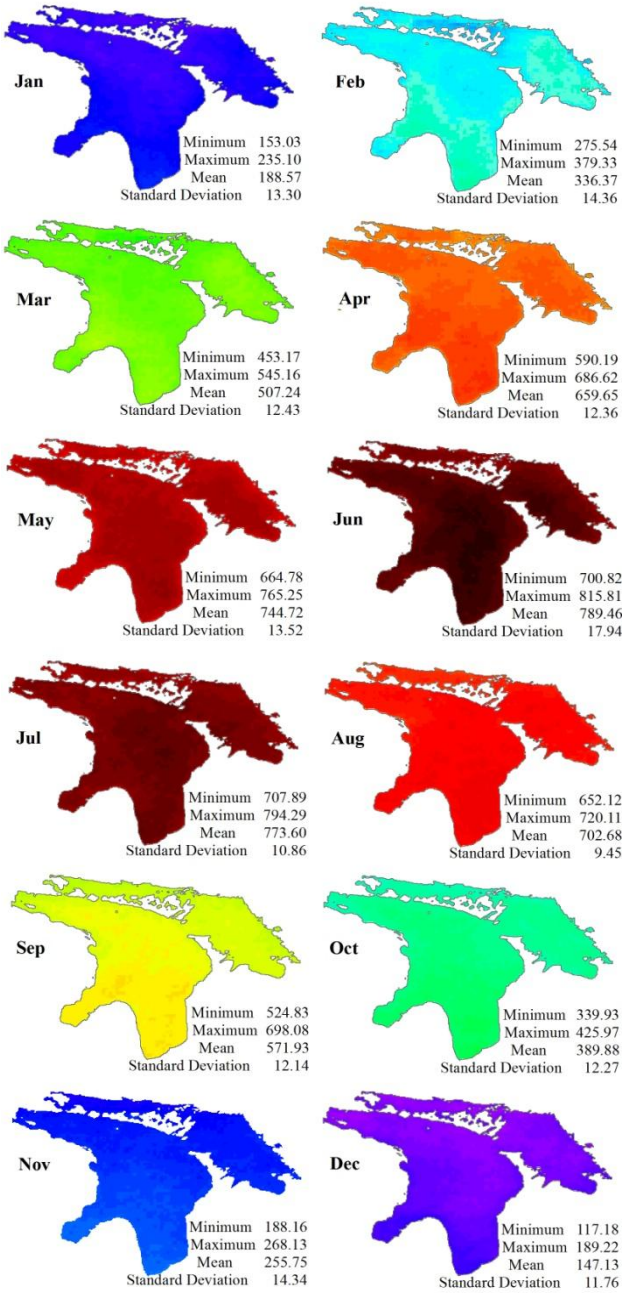


Figure 5. Spatial distribution of monthly average net radiation ($Wm^{-2}$) from 2002 – 2012.

## C. *Change of net radiation*

Time series of daily instantaneous radiation at the lake's surface in $Wm^{-2}$ and the trend line for the 11-years (2002–2012) period were presented in Fig. 6. The trend exhibited a statistically significant (95% confidence level) decline in incoming shortwave and an increase in incoming long-wave and outgoing long-wave radiations. The outgoing shortwave showed a slight upward trend, however it was not statistically significant.

Net radiation, according to changes of its four components, shows a significant decline of 1.09 W $m^{-2}$ per year corresponding to 12.04 W $m^{-2}$ for the entire period 2002-2012. The decrease in surface incident solar radiation followed by an increase in outgoing long wave radiation contributed to this observed trend. There was a

slight increase in downwelling long-wave radiation, which was relatively small compared to the decrease in incoming shortwave radiation. The following are details of the three net radiation components (incoming shortwave, incoming long-wave, and outgoing long-wave) that had a significant contribution to the trends in net radiation.

Incoming solar radiation over the lake had a significant downward trend of 1.38 W $m^{-2}$ per year corresponding to 15.25 W $m^{-2}$ for the entire period (2002-2012). This result in agreement with Hinkelman *et al*. [25] who observed a decline in solar surface radiation in North America during the period 1998-2004 and similar to Liepert [26] who observed a reduction of 19 W $m^{-2}$ in surface solar radiation in the United States between the 1960s and the 1980s.

This study used 1367 W $m^{-2}$ solar constant, therefore, the variations in incidence solar radiation that reached the lake surface cannot be explained by changes in the luminosity of the sun. Therefore, the changes in incoming shortwave radiation had to be a result of variations in the atmosphere transparency, which controlled by the occurrence of cloud, aerosols, and water vapor. From our observation, there were slight decrease in cloud cover and its optical thickness over the lake, which would supposedly allow more incoming shortwave radiation to reach the surface. However, our results showed a decrease in the incoming solar radiation indicating a reduction in amount of cloud cover could not be accounted for as a factor lead to increase in surface shortwave radiation. This corresponds to the study of Qian *et. al*. [27] and Norris and Wild [28] who reported that changes in cloud cover effect can be detected on an inter-annual basis, however, their influence to the long term trend of incoming solar radiation is not constantly noticeable.

The possible reason for the reduction in surface incoming shortwave radiation was the absorption of shortwave radiation by water vapor in the air. This study observed an increase in vapor pressure (Fig. 7), which in-turn could result in a decrease in incident surface solar radiation. This is a reasonable explanation, because water vapor is the most absorbing gas in the atmosphere [29] and it has a number of absorption bands in the shortwave spectral regions where the most intensive bands are the bands in ultraviolet and near infrared. Although the absorption band in visible ranges are very small, but are present [30] within the wavelength between 0.572-0.703 µm [31]. Our study results corresponded to the study of Arking [32] who claimed that water vapor is the most dominant factor in the atmospheric absorption of shortwave radiation. Braswell and Lindzen [33] also found that water vapor in clear air absorbs significant amount of solar radiation.

The incoming long-wave radiation had an increase of 1.13 $Wm^{-2}$ per year corresponding to about 12.45 $Wm^{-2}$ for the 11 years. The change in incoming long-wave is generally influenced by the change of temperature and humidity of the atmosphere and by the cloud covers [34]. As mentioned earlier, cloud cover and cloud optical thickness were slightly decreasing over the study period, thus, the increase in incoming long-wave radiation was driven by the long-term increase in vapor pressure and air temperature. Outgoing long-wave had also an upward trend of 0.84 $Wm^{-2}$ per year corresponding to about 9.23 $Wm^{-2}$ for the entire study period (2002-2012). This increase was mainly due to the increase of lake surface water temperature.

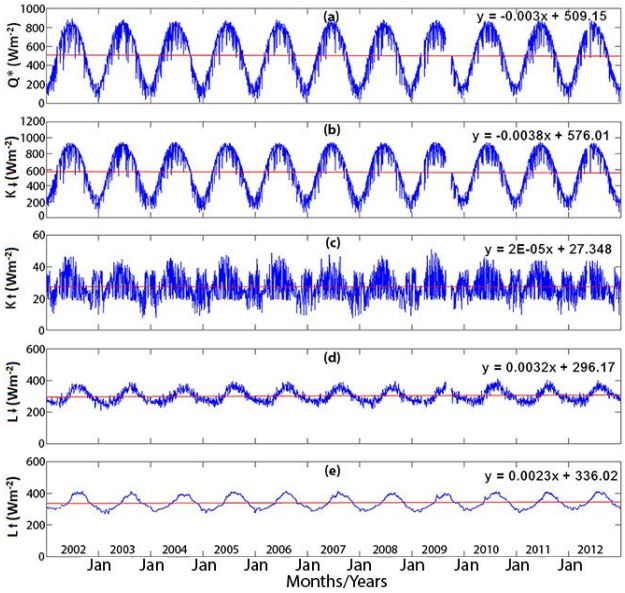


Figure 6. Time series of instantaneous net radiation (a), incoming shortwave (b), outgoing shortwave (c), incoming longwave (d), and outgoing long-wave (e) at the lake's surface in W $m^{-2}$ and the trend line for the 11-years (2002–2012).

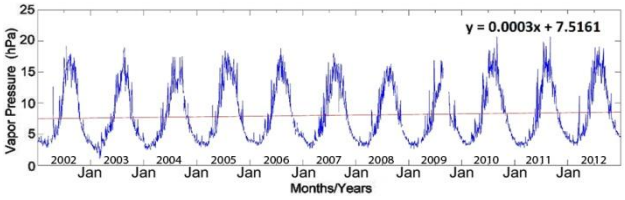


Figure 7. Time series of instantaneous vapor pressure (hPa) and the trend line for the 11-years (2002–2012).

## V. Summary and Conclusion

Inter-annual and long-term spatiotemporal variability of surface net radiation was estimated from MODIS data using a four-component approach. A good correlation was found between the parameters calculated from satellite data and in situ observations. The correlation coefficient was 0.95 for outgoing long-wave radiation, whereas, incoming radiation (both shortwave and long-wave) had a correlation coefficient of approximately 0.60 due to the difference in spatial sampling between satellite and ground station. No validation was carried out for the outgoing shortwave radiation, because of the contamination of the outgoing signal from the lighthouse base and no other ground measurements were available.

The spatial distribution of the net radiation and its four components showed temporal and spatial heterogeneities. The study found that the decrease in

incoming shortwave radiation, the increase in incoming and outgoing long-wave radiation were statistically significant over the 11-yr observation period. Outgoing shortwave has a small increasing trend, but it was not statistically significant. The instantaneous net radiation was dominated by incident shortwave radiation, however, it declined by 1.09 W $m^{-2}$ per year corresponding to about 12.04 W $m^{-2}$ for the entire period (2002-2012). This was mainly due to the significant decrease in incoming shortwave radiation, followed by increase in outgoing long-wave radiation. The positive trend of outgoing long-wave radiation was obviously a result of the increase of surface water temperature. The possible reason for reduction of surface incoming shortwave radiation was mainly the increase of energy absorption by water vapor in the atmosphere.

Use of satellite data for computing the net radiation parameters presented in this paper will allow a better understanding of spatial distribution and improve spatial resolution, and analysis at wide areas. The information provided in this study can be an important parameter for input to the numerical models for assessing the magnitude of surface energy balance.

## REFERENCES


[1] C.A. Federer, "Spatial variation of net radiation, albedo and surface temperature of forests," *Journal of Applied Meteorology*, vol. 7, pp. 789-795, October 1968.

[2] G. Bisht, V. Venturini, S. Islam, and L. Jiang, "Estimation of the net radiation using MODIS (Moderate Resolution Imaging Spectroradiometer) data for clear sky days," *Remote Sensing of Environment*, val. 97, pp. 52-67, July 2005

[3] Z. Sun, M. Gebremichael, Q. Wang, J. Wang, T.W. Sammis, A. Nickless A2013. "Evaluation of clear-sky incoming radiation estimating equations typically used in remote sensing evapotranspiration algorithms", *Remote Sensing*, vol. 5, pp. 4735-4752, September 2013

[4] C.R. Dugual, "An approach to the estimation of surface net radiation in mountain area using remote sensing and digital terrain data," *Theoretical and Applied Climatology*. Vol.55, pp. 55-68, January 1994

[5] R.M.L Mckay, B.F.N. Beall, G.S, Bullerjahn, W.C. Woityra, "Winter limnology on the Great Lakes: The role of the U.S. Coast Guard," *Journal of Great lakes Research*. Vol. 37, pp. 207-210, March 2011.

[6] B.O. Oyserman, W.C. Woityra, G.S. Bullerjahn, B.F.N Beall, R.M.L. Mckay, "Collecting winter data on U.S. Coast Guard icebreakers," *EOS, Transactions American Geophysical Union*. Vol. 93, pp. 105-106, March 2012

[7] S. Swenson, J. Wahr, "Monitoring the water balance of Lake Victoria, East Africa, from space," *Journal of Hydrology*, vol. 370, pp. 163–176, May 2009.

[8] W. Wang, S. Liang,. "Estimation of high-spatial resolution clear-sky longwave downward and net radiation over land surfaces from MODIS data," *Remote Sensing of Environment*, vol. 113, pp. 745-754, 2009

[9] C.A. Santos, R.L. Nascimento, T.V. Rao, A.O. Manzi, "Net radiation estimation under pasture and forest in Rondônia, Brazil, with TM Landsat 5 images," *Atmosfera.* Vol. 24, 234-446, 2011

[10] G. Bisht, R.L. Bras, "Estimation of net radiation from the MODIS data under all sky conditions: Southern Great Plains case study". *Remote Sensing of Environment*. vol. 114, pp. 1522-1534, 2010

[11] Y. Jin, J.T. Randerson, M.L. Goulden, "Continental-scale net radiation and evapotranspiration estimated using MODIS satellite observation," *Remote Sensing of Environment*, vol. 115, 2302-2319, September 2011.

[12] H.Y. Kim, S. Liang, "Development of hybrid method for estimating land surface shortwave net radiation from MODIS," *Remote Sensing of Environment*, vol. 114, pp. 2393-2402, 2010

[13] B.Tang, Z.L. Li, "Estimation of instantaneous net surface longwave radiation from MODIS cloud-free data," *Remote Sensing of Environment*. vol. 112, pp. 3482-3492, 2008.

[14] J. MacDonagh-Dumler, V. Pebbles, J. Gannon, "Great Lakes (North American) – experience and lessons learned brief," in: *ILEC. 2005. Managing Lakes and their Basins for Sustainable Use: A Report for Lake Basin Managers and Stakeholders*. International Lake Environment Committee Foundation: Kusatsu, Japan, pp. 179-191, 2005

[15] W.M. Schertzer, R.A. Assel, D. Beletsky, T.E. Croley II, B. M. Lofgren, J.H. Saylor, et al., "Lake Huron climatology, inter-lake exchange and mean circulation," *Aquatic Ecosystem Health & Managemen.*vol. 11, pp. 144 – 152, June 2008

[16] *MODIS Reprojection Tool (MRT).* User's Manual, Release 4.1, Land Processes DAAC, USGS Earth Resources Observation and Science (EROS) Center, 2011

[17] M. Nunez, J.A. Davies, P.J. Robison, "Suface albedo at a tower site in Lake Ontario," *Boundary-Layer Meteorology*, vol. 3, pp 77-86, Febuary 1972.

[18] P.D. Blanken, W.R. Rouse, A.D. Culf, C. Spence, L.D. Boudreau, J.N. Jasper, et al, "Eddy covariance measurements of evaporation from Great Slave Lake, Northwest Territories, Canada, " Water Resources Research, vol. 36, pp. 1069-1077, April, 2000

[19] W.J. Zillman, "A study of some aspects of the radiation and heat budgets of the southern hemisphere oceans, meteorological study 26," Canberra, Australia, 1972

[20] R.R. Roger, M.K. Yau, *A Short Course in Cloud Physics*. 3rd ed E, Pergamon Press. 1989:

[21] A. Slingo, "A GCM parameterization for the shortwave radiative properties of water clouds," *Journal of Atmospheric Science*," vol. 46, pp. 1419-1427, November 1989

[22] A.J. Prata, "A new long-wave formula for estimating downward clear sky radiation at the surface, " Quarterly Journal Royal Meteorological Society, vol. 122, pp 1127-1151, July 1996

[23] D.J. Schwab, G.A. Leshkevich, G.C. Muhr, "Automated mapping of surface water temperature in the Great Lakes," *Journal of Great Lakes Research*, Vol. 25, pp. 468 – 481, 1999.

[24] C. Coll, V. Caselles, J.M. Galve, E. Valor, R. Niclòs, J. M. Sanchez, et al., "Ground measurements for the validation of land surface temperatures derived from AATSR and MODIS data," *Remote Sensing of Environment*. Vol. 97, pp 288–300, August 2005.

[25] L.M. Hinkelman, P.W. Stackhouse, B.A. Wielicki, T. P. Zhang, S.R. Wilson, "Surface insolation trends from satellite and ground measurements: Comparisons and challenges," *Journal of Geophysical Research*. Vol. 114, D00D20, August 2009, doi:10.1029/2008JD011004

[26] B.G. Liepert, "Observed reductions of surface solar radiation at sitesin the United States and worldwide from 1961 to 1990," *Geophysical Research Letter*, Vol. 29, 1421, May 2002. doi:10.1029/2002GL014910.

[27] Y. Qian, D.P. Kaiser, L.R. Leung, M. Xu, "More frequent cloud-free sky and less surface solar radiation in China from 1955 to 2000," *Geophysical Research Letters*, vol. 33, L01812, January 2006, doi:10.1029/2005GL024586

[28] J.R. Norris, M. Wild, "Trends in aerosol radiative effects over Europe inferred from observedcloud cover, solar "dimming" and solar "brightening"," *Journal of Geophysical Research*, vol. 112, April 2007, D08214,doi:10.1029/2006JD007794.

[29] J.L. Monteith, M.H. Unsworth, *Principles of Environmental Physics*, 3rd ed, Amsterdam; Boston: Elsevier, 418 p, 2008.

[30] K.N. Liou, *An Introduction to Atmospheric Radiation, Vol 84*, 2nd ed, 583 p, 2002

[31] K.V. Kondratyev, *Radiation in the Atmosphere Vol. 12*, Academic Press Inc, 910 p,1969

[32] A. Arking, "Absorption of solar energy in the atmosphere: discrepancy between model and observations," *Science*, Vol. 273, pp. 779-781, August 1996.

[33] W.D. Braswell, R.S. Lindzen, "Anomalous short wave absorption and atmospheric tides," *Geophysical Research Letters*. Vol. 25, pp 1293-1296, May 1998.

[34] J.E. Sicart, R. Hoch, P. Ribstein, J.P. Chazarin, "Sky longwave radiation on tropical Andean glaciers: Parameterization and sensitivity to atmospheric variable," *Journal of Glaciology*, vol. 56, pp. 854-860, 2010, doi:10.3189/002214310794457182